

Electronic supplementary information (ESI)

FRET-mediated pH responsive dual fluorescent nanoparticles prepared via click chemistry

K. Ouadahi, K. Sbargoud, E. Allard and C. Larpent*

Correspondence to: larpent@chimie.uvsq.fr

Table of Contents

	pages
- Materials and Methods; Synthesis of functionalized nanoparticles	2-4
- Fig. S.1: IR spectra of NP-N ₃ and fluorescent dual NPs NP-DF1	5
- Fig. S.2: IR spectra of NP-N ₃ and dansyl-functionalized NPs NP-D	6
- Fig. S.3: IR spectra of NP-N ₃ and fluorescein-functionalized NPs NP-F	7
- Fig. S.4: Absorption and fluorescence spectra of NP-F at different pH	8
- Fig. S.5: Fluorescence spectra of Dansyl-functionalized NP-D at different pH	9
- Fig. S.6: Overlap of the absorption and fluorescence spectra of Dansyl- and Fluorescein-functionalized NPs : NP-D NP-F	10
- Fig. S.7: Absorption spectra of dual NPs NP-DF1 at different pH	11
- Fig. S.8: Fluorescence spectra of Dual NPs NP-DF1 at different pH values upon excitation of fluorescein at 500 nm	12
- Fig. S.9: Fluorescence spectra of Dual NP-DF1 upon excitation at 340 nm at different pH values	13
- Fig. S.10: Absorption spectra of Dual NPs NP-DF1 and NP-DF2 at neutral pH	14
- Fig. S.11: Fluorescence spectra of Dual NP-DF2 upon excitation at 340 nm at different pH values	15
- Förster's distance R_0 and FRET efficiency	16
- Fig. S.12: Variations of the emission intensity at 475 nm and FRET efficiency vs pH for dual NP-DF1 and NP-DF2	19
- Fig. S.13: Calculated variations of E vs pH in NP-DF1.	19
- Fig. S.14: Calculated variations of the relative emission of dansyl vs pH in NP-DF1.	20
- Fig. S.15: Calculated variations of E vs pH in NP-DF2.	21
- Fig. S.16: Calculated variations of the relative emission of dansyl vs pH in NP-DF2.	22

Materials and Methods

Fluorescein and dansyl derivatives **F** and **D** were prepared according to the reported procedures.^{S1,S2} Dodecyltrimethylammonium bromide (DTAB, 98% from Fluka) and other reagents were of commercial origin and used without purification. Monomers were freed of inhibitors before polymerization. Vinylbenzylchloride (VBCl, mixture of meta and para isomers 70/30, 95% from Aldrich), and divinylbenzene (DVB, mixture of meta and para isomers, 80% from Fluka) were passed through a LC-Si Solid Phase Extraction tube. Styrene (99% from Acros) was distilled under reduced pressure. MilliQ water was used for microemulsion polymerization and sample dilution.

Elemental analyses and IR spectra of the polymer particles. The polymer was flocculated by adding 20 mL of methanol to 2 g of suspension and then separated by centrifugation (8000 rpm, 15 min). The resulting precipitate was extensively washed with demineralised water and methanol (stirring for 1 hour followed by centrifugation) and finally dried at 50°C until constant weight.

The chemical composition of the NPs was deduced from elemental analyses (obtained from the Service de Microanalyse, ICSN, Gif/Yvette, France) of the isolated and purified polymer.

IR spectra (KBr pellets) of the isolated and purified polymers were recorded on a Nicolet Impact 400D spectrometer.

DLS analyses. The sizes of the nanoparticles were determined in solution by QELS with a Brookhaven 90 plus. The data were analysed by the exponential sampling method. The samples were diluted 100 times in MilliRo water and filtered through a 0.22 µm micropore filter before analysis. The average diameter was calculated by the cumulants analysis.

AFM analyses. AFM measurements were made using tapping mode operation with a Digital Instrument 3100 and a Nanoscope IIIa controller. Tapping mode etched silicon probes from Veeco (TESP-SS, spring constant k_0 : 20-80 N/m and constant force f_0 : 300-371 kHz) with a 3.5 - 4.5 nm radius of curvature were used. Mica substrates were cleaved to produce a defect-free smooth surface prior to sample deposition. The suspensions were diluted 4×10^4 times in water (final concentrations of NPs: 1×10^{-3} g.L⁻¹). 10 µL of the dilute solutions was deposited on 9 mm Mica disks and allowed to dry at room temperature for 12 hours.

UV-Visible absorption measurements. Absorption spectra were recorded on a Perkin-Elmer spectrophotometer UV/Vis/NIR Lambda 19. A 1cm path quartz cell was used and the measurements were done from 200 nm to 800 nm. Absorption spectra of fluorescent NPs were acquired on samples diluted 50 to 100-fold in aqueous solution of DTAB 0.5 wt%.

Fluorescence measurements. Steady-state fluorescence measurements were performed on a spectrofluorimeter FluoroMax-3 equipped with a 150W Xenon lamp and a slit width of 5 nm. A 1 cm path quartz cell was used for the measurements. For all measurements the maximum of absorbance of the diluted samples is less than 0.1 to avoid re-absorption artefacts. Fluorescence spectra of fluorescent NPs were acquired on samples diluted 500 to 1000-fold in aqueous solution of DTAB 0.5 wt%.

pH titration procedure. The aqueous suspensions of NPs were diluted in 6 mM phosphate buffer at different pH values containing 0.5 wt % of DTAB. The pHs below 5.0 were adjusted by adding aliquots of 10 µL of HCl (1M). The pH values were checked using a digital pH meter (Consort C832) equipped with a pH microelectrode (Fisherbrand). Standard buffers (pH 10.01, 7.01, 4.01) were used for calibration.

Synthesis of functionalized nanoparticles

Primary reactive chlorobenzyl-functionalized nanoparticles NP-Cl. The aqueous suspension of starting chlorobenzyl-functionalized nanoparticles NP_{Cl} was prepared using the previously described procedure.^{S3} Briefly, a microemulsion was prepared by progressive addition, upon gentle magnetic stirring, of a mixture of monomers (styrene / divinylbenzene / vinylbenzylchloride: 33.6 / 34.6 / 11.9 mmol, respectively) and 2,2-dimethoxy-2-phenyl acetophenone (initiator, 1.3 mmol) to 220 g of a 15 wt% solution of dodecyltrimethylammonium bromide (DTAB) in demineralized water. The resulting microemulsion was degassed with nitrogen for 30 minutes and the polymerization was then carried out under white light irradiation using two 60 W lamps at room temperature under nitrogen overnight. Stable translucent nanolatex was obtained.

Polymer elemental analysis: C, 84.89; H, 7.26; Cl, 3.10%.

Mean diameter (QELS): 15 nm (PDI: 0.036)

IR (KBr): 3084, 3059, 3028, 2921, 2853, 1938, 1863, 1800, 1701, 1605, 1513, 1494, 1448, 1362, 1223, 1152, 986, 900, 841 cm⁻¹.

Azide-functionalized nanoparticles NP-N₃. Azide-coated nanoparticles NP_{N₃} were prepared by adding an aqueous solution of sodium azide (3.39 g in 10 mL of water) to 100 g of the crude suspension of NP-Cl (pH of the suspension was previously adjusted to 7.5). The resulting suspension was stirred at room temperature for one week. The excess of sodium azide was then removed by dialysis through a porous cellulose membrane (MWCO 12000-14000D) toward an aqueous solution of DTAB (15 wt%) leading to a stable translucent aqueous suspension of azide-functionalized nanoparticles (NP_{N₃}).

Polymer elemental analysis: C, 84.77; H, 7.77; N, 1.91%.

Mean diameter (QELS): 16 nm (PDI: 0.037).

IR (KBr): 3080, 3055, 3022, 2917, 2852, 2094 (-N₃), 1937, 1867, 1800, 1698, 1600, 1509, 1495, 1448, 1346, 1263, 1070, 1030, 987, 907, 834 cm⁻¹.

Preparation of Dansyl-functionalized nanoparticles NP-D. Dansyl derivative **D** (0.0678g, 0.235 mmol, about 1eq. per azide) was added to 12 g of the aqueous suspension of NP-N₃. The mixture was stirred at room temperature until complete solubilisation of **D** (about 30 min). Then, 1 mL of a freshly prepared aqueous solution of CuSO₄ (0.0151g, 0.095 mmol) and sodium ascorbate (0.210g, 1.06 mmol) was added. The resulting suspension was stirred at room temperature for 4 days. The suspension was dialyzed against aqueous solutions of DTAB (15 wt% then 5 wt%) using an ultrafiltration device (Vivascience, Vivaspin concentrator 20, 50 000 MWCO PES). The process was repeated until no dansyl derivative was detected in the filtrate.

Polymer elemental analysis: C, 83.44; H, 7.11; N, 2.51; S, 1.02%.

Mean diameter (QELS): 17 nm (PDI: 0.101)

IR (KBr): 3082, 3059, 3025, 2920, 2847, 2787, 2100, 1940, 1872, 1801, 1629, 1604, 1512, 1496, 1450, 1330, 1264, 1233, 1165, 1145, 1074, 1045, 989, 906, 841 cm⁻¹.

Preparation of Fluorescein functionalized nanoparticles NP-F. Fluorescein derivative **F** (0.087g, 0.196 mmol, about 1eq. per azide) was added to 10g of the aqueous suspension of NP-N₃. The pH was adjusted with NaOH (1M) until complete solubilisation of **F** (pH close to 7). Then, 1 mL of a freshly prepared aqueous solution of CuSO₄ (0.0125g, 0.079 mmol) and sodium ascorbate (0.175g, 0.88 mmol) was added. The resulting suspension was stirred at room temperature for 7 days. The suspension was

dialyzed against aqueous solutions of DTAB (15 wt% then 5 wt%) using an ultrafiltration device (Vivascience, Vivaspin concentrator 20, 50 000 MWCO PES). The process was repeated until no fluorescein derivative was detected in the filtrate.

Polymer elemental analysis: C, 81.26; H, 7.24; N, 1.86; S, 0.22% (*under precision limit*).

Mean diameter (QELS): 16 nm (PDI: 0.091)

IR (KBr): 3082, 3059, 3025, 2920, 2849, 2094, 1943, 1864, 1682, 1631, 1599, 1511, 1489, 1449, 1352, 1247, 1156, 1111, 1028, 989, 903, 835 cm⁻¹.

Preparation of Dual nanoparticles NP-DF1 (D/F ratio = 4 to 4.5/1). Fluorescein derivative **F** (0.240 g, 0.54 mmol) was added to the aqueous suspension of NP-N₃ (20g, polymer content 4.5 wt%, azide content of 0.502 mmol/g of polymer). The pH was adjusted with NaOH (1M) until complete solubilisation of **F** (pH close to 7). Then, 1 mL of a freshly prepared aqueous solution of CuSO₄ (0.068g, 0.43 mmol) and sodium ascorbate (0.954g, 4.8 mmol) was added. The resulting suspension was stirred at room temperature for 5 days. Dansyl derivative **D** (0.156 g, 0.54 mmol) was then added to the crude suspension of **NP-F**. The mixture was stirred at room temperature until complete solubilisation of **D** (1h). A freshly prepared aqueous solution (1 mL) of CuSO₄ (0.068g) and sodium ascorbate (0.954g) was added. The reaction mixture was stirred at room temperature for 6 days. The suspension was dialyzed against aqueous solutions of DTAB (15 wt% then 5 wt%) using an ultrafiltration device (Vivascience, Vivaspin concentrator 20, 50 000 MWCO PES). The process was repeated until no fluorescein and dansyl derivatives were detected in the filtrate.

Polymer elemental analysis: C, 77.85; H, 6.44; N, 2.48; S, 1.25 %.

Mean diameter (QELS): 18 nm (PDI: 0.061)

IR (KBr): 3080, 3061, 3024, 2922, 2850, 2096, 1599, 1493, 1452, 1331, 1233, 1158, 1075, 902, 863 cm⁻¹

Preparation of Dual nanoparticles NP-DF2 (D/F ratio =13/1). These particles were prepared using the procedure described above using 30 g of aqueous suspension of NP-N₃, 0,06g **F**, 0,154g **D**, 0.043 g CuSO₄ and 0.6 g sodium ascorbate.

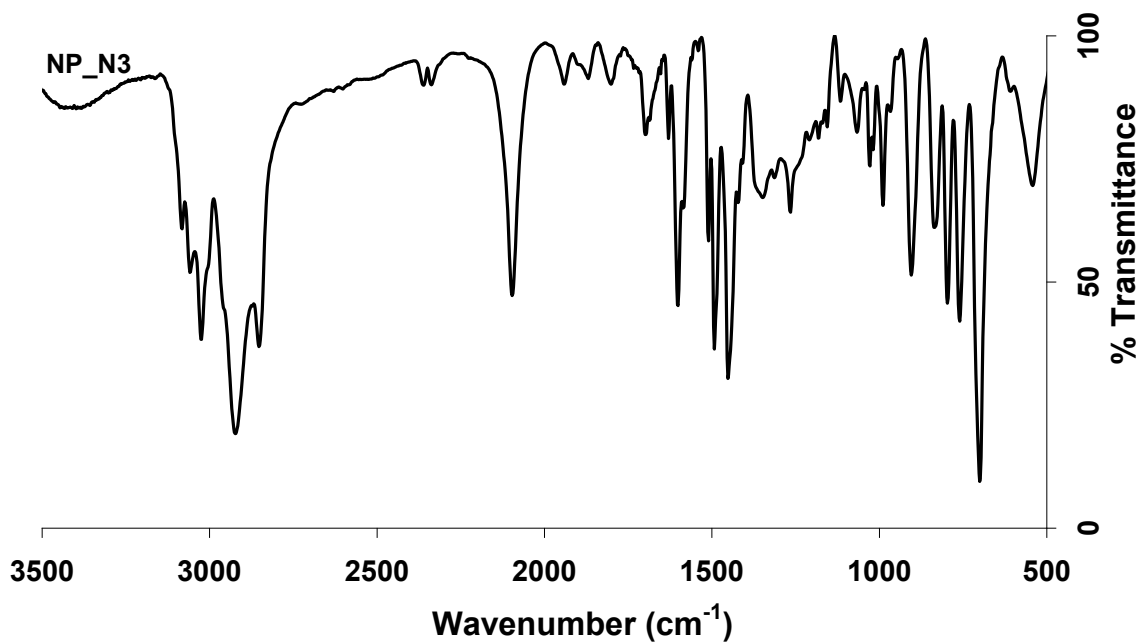
Polymer elemental analysis: C, 81.68; H, 7.19; N, 2.49; S, 1.01 %.

Mean diameter (QELS): 19 nm (PDI: 0.1).

IR : 3082, 3056, 3024, 2919, 2850, 2785, 2094, 1685, 1598, 1511, 1493, 1453, 1323, 1233, 1160, 903, 795, 759, 697.

Figure S.1 : IR spectra of NP-N₃ (a) and fluorescent dual NPs NP-DF1 (b)

a) NP-N₃



b) Dual NP-DF1

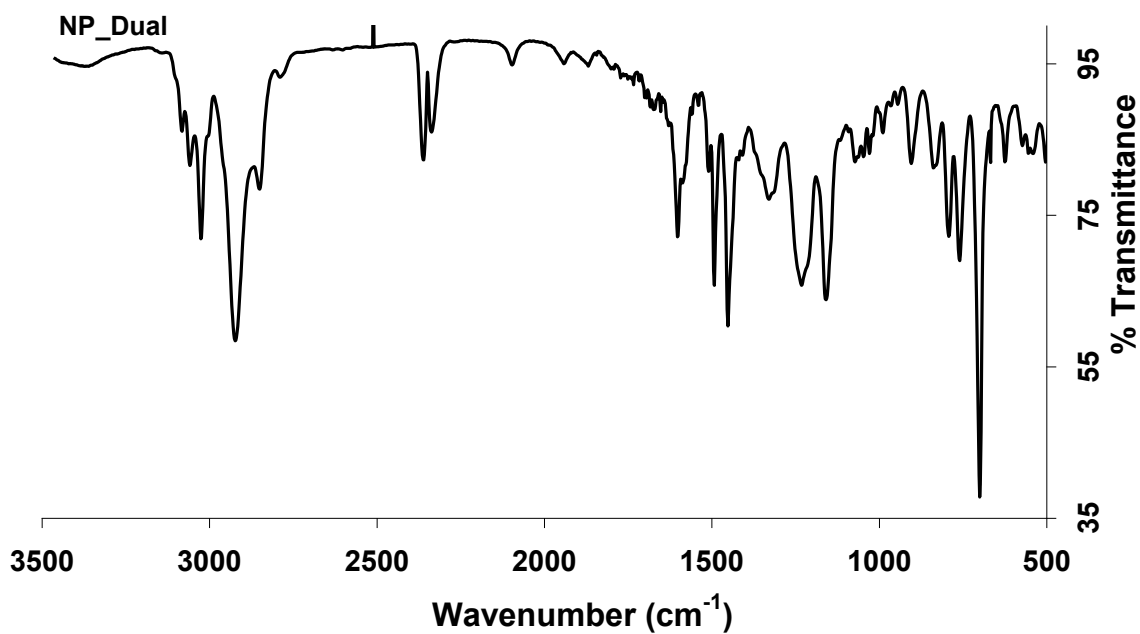
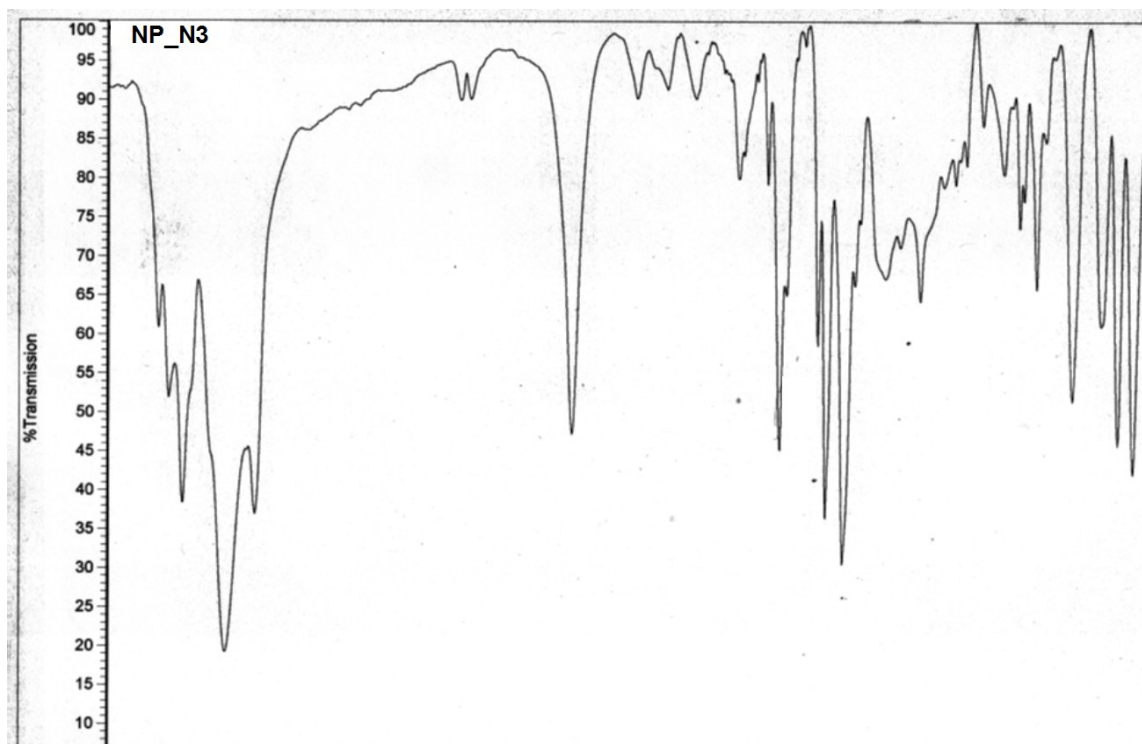


Figure S.2 : IR spectra of NP-N₃ (a) and dansyl-functionalized NPs NP-D (b)

a) NP-N₃



b) NP-D

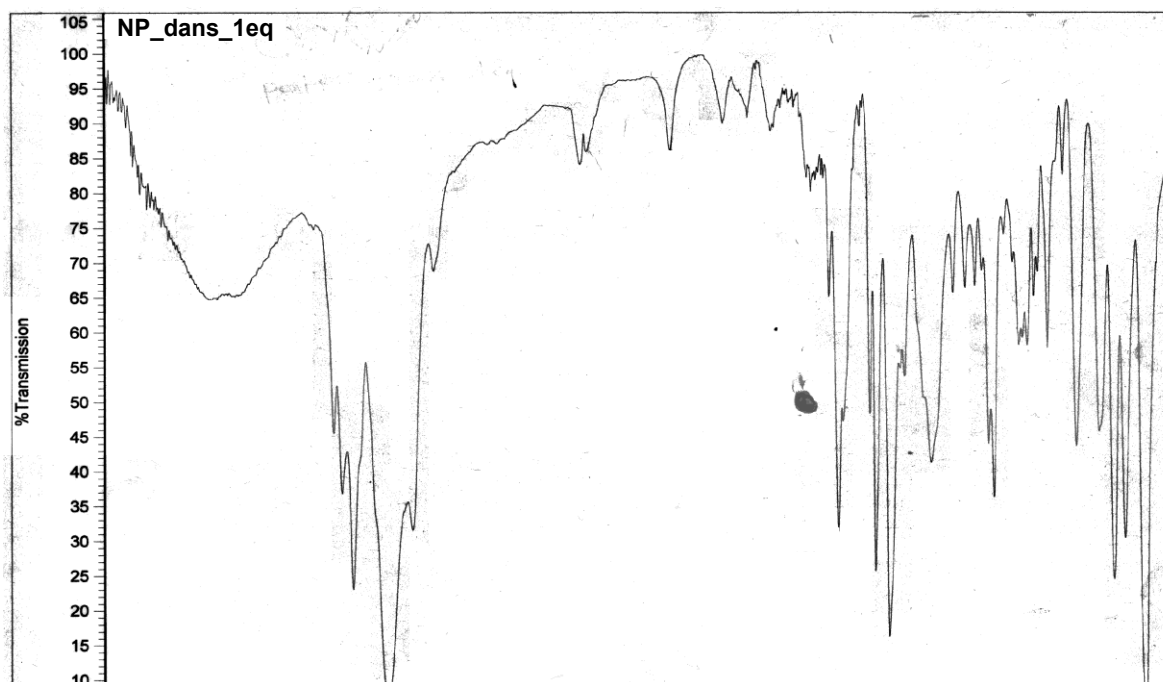
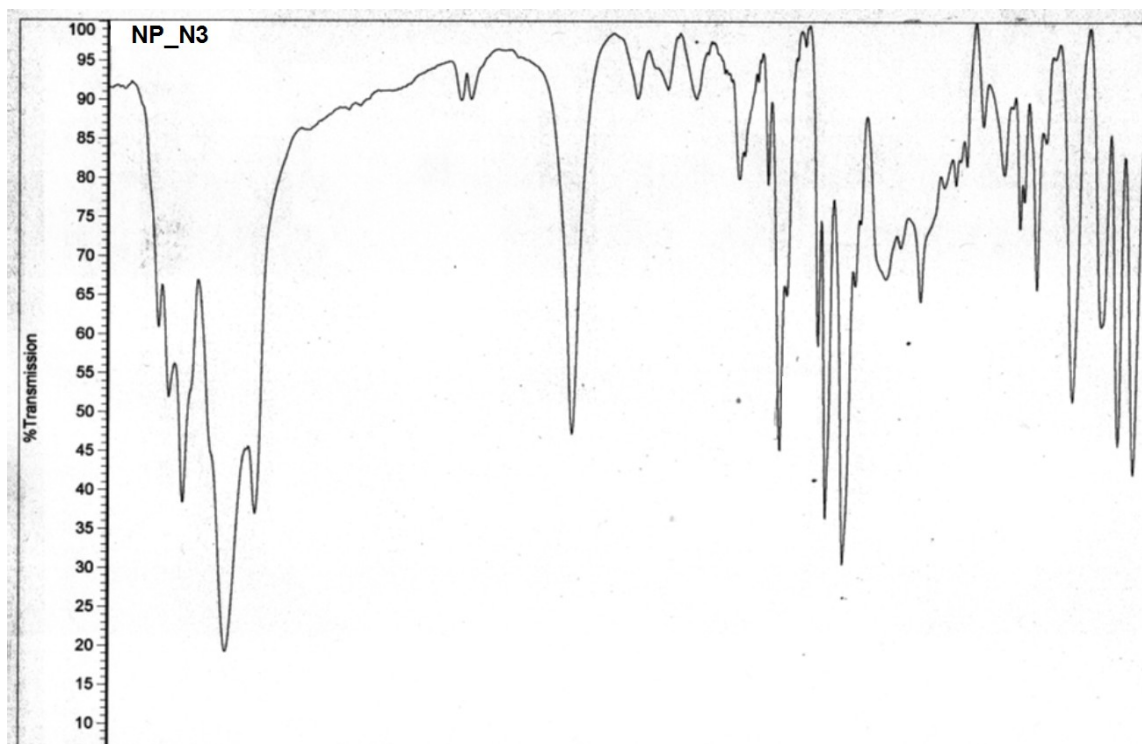


Figure S.3 : IR spectra of NP-N₃ (a) and fluorescein-functionalized NPs NP-F (b)

a) NP-N₃



b) NP-F

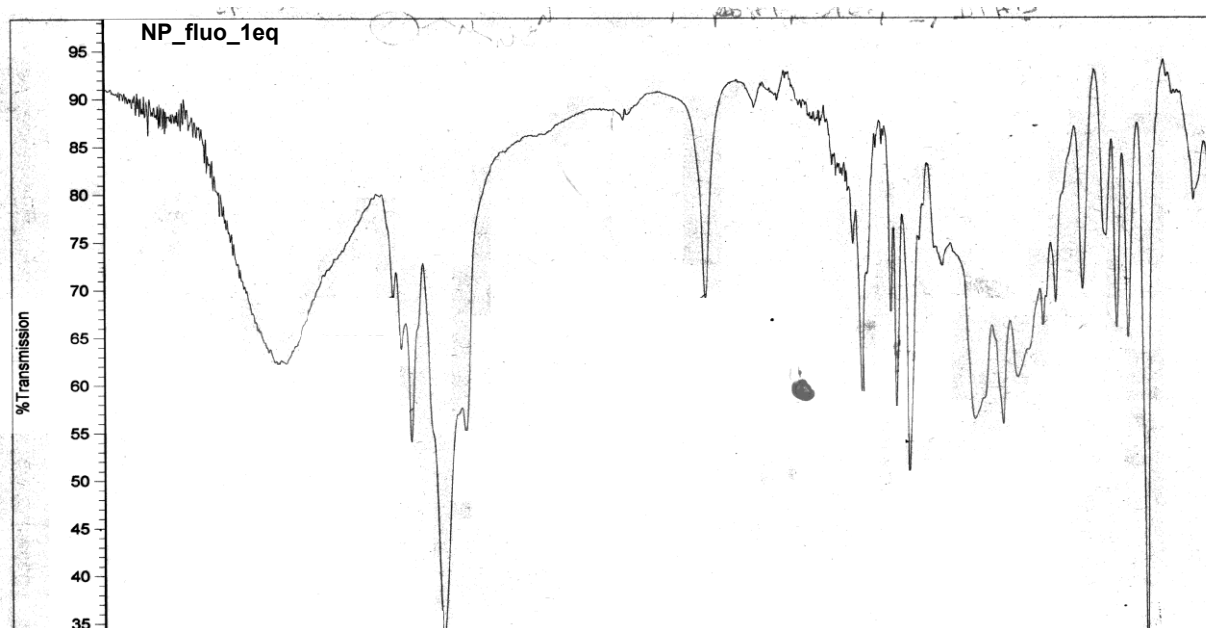
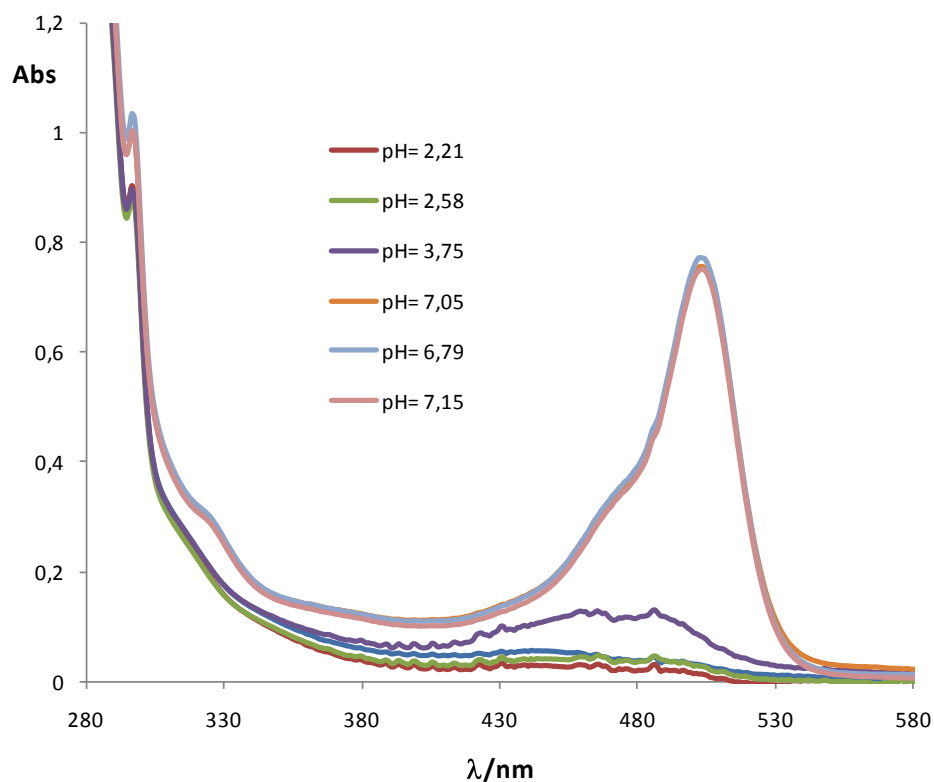
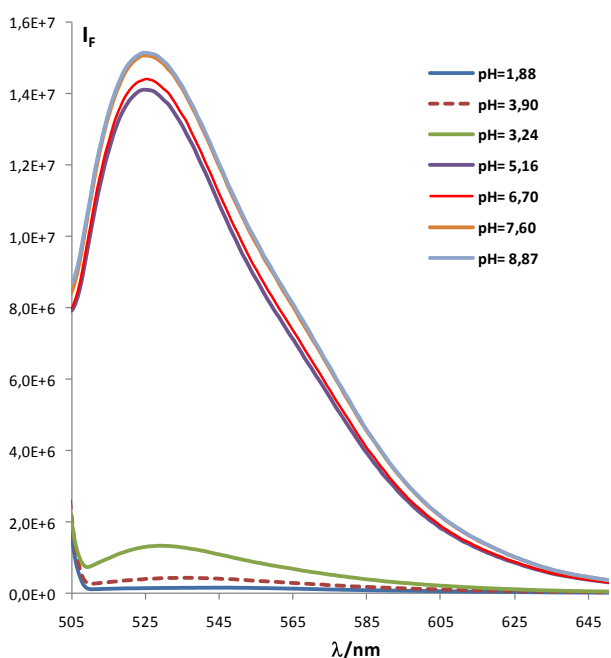


Figure S.4 : Absorption and fluorescence spectra of NP-F at different pH

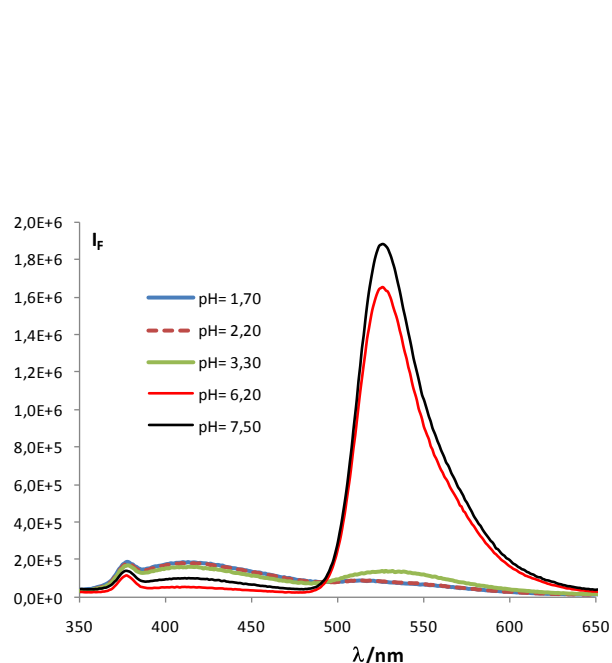
a) Absorption spectra (dilution 80, DTAB 0.5 wt %)



**(b) Fluorescence emission spectra
Excitation at 500 nm (dilution 800 in DTAB 0.5wt %)**



**(c) Fluorescence emission spectra
Excitation at 340 nm (dilution 800 in DTAB 0.5wt %)**



The emission intensity is about 10 times higher upon excitation at 500nm than upon excitation at 340 nm

Figure S.5 : Fluorescence spectra of Dansyl-functionalized NP-D at different pH (excitation 340 nm, suspension diluted 1000 times in DTAB 0.5 wt%)

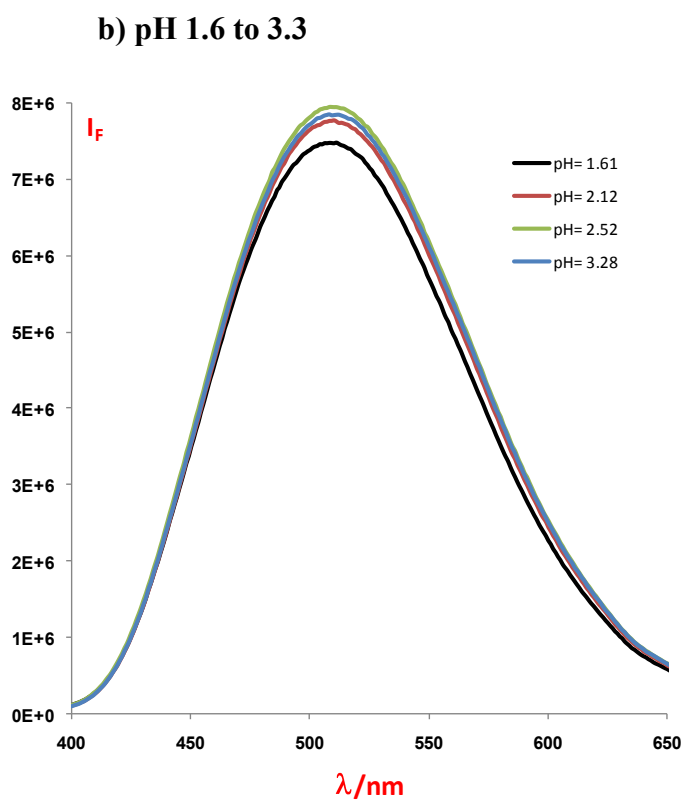
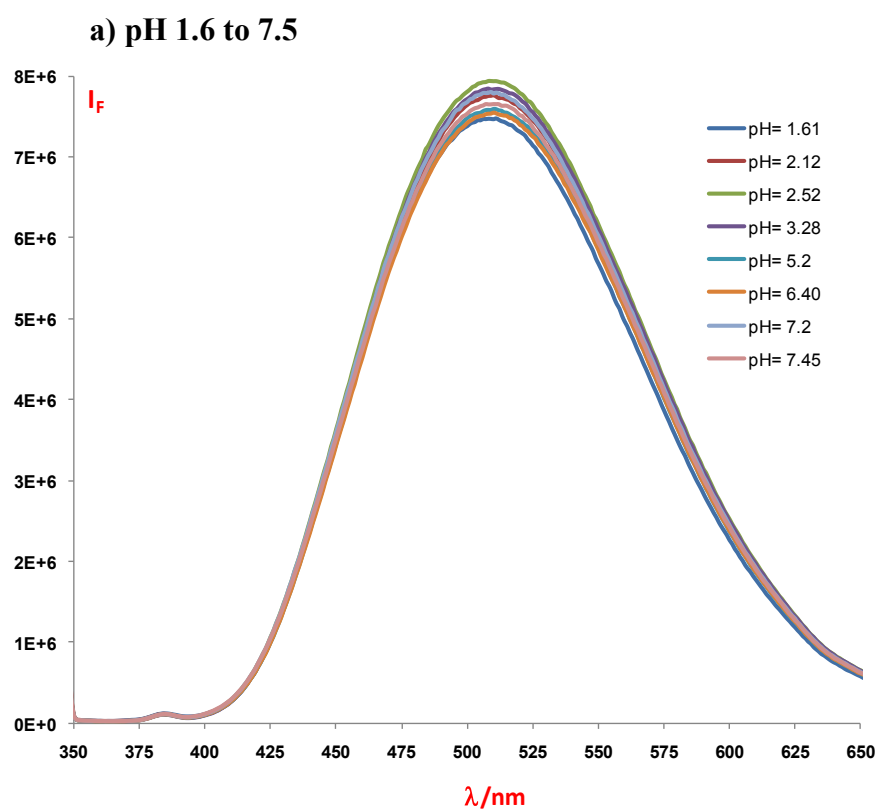


Figure S.6 : Absorption and Fluorescence spectra of Dansyl-functionalized NP-D and Fluorescein-functionalized NP-F showing the overlap of the emission of dansyl and the absorption of fluorescein base.

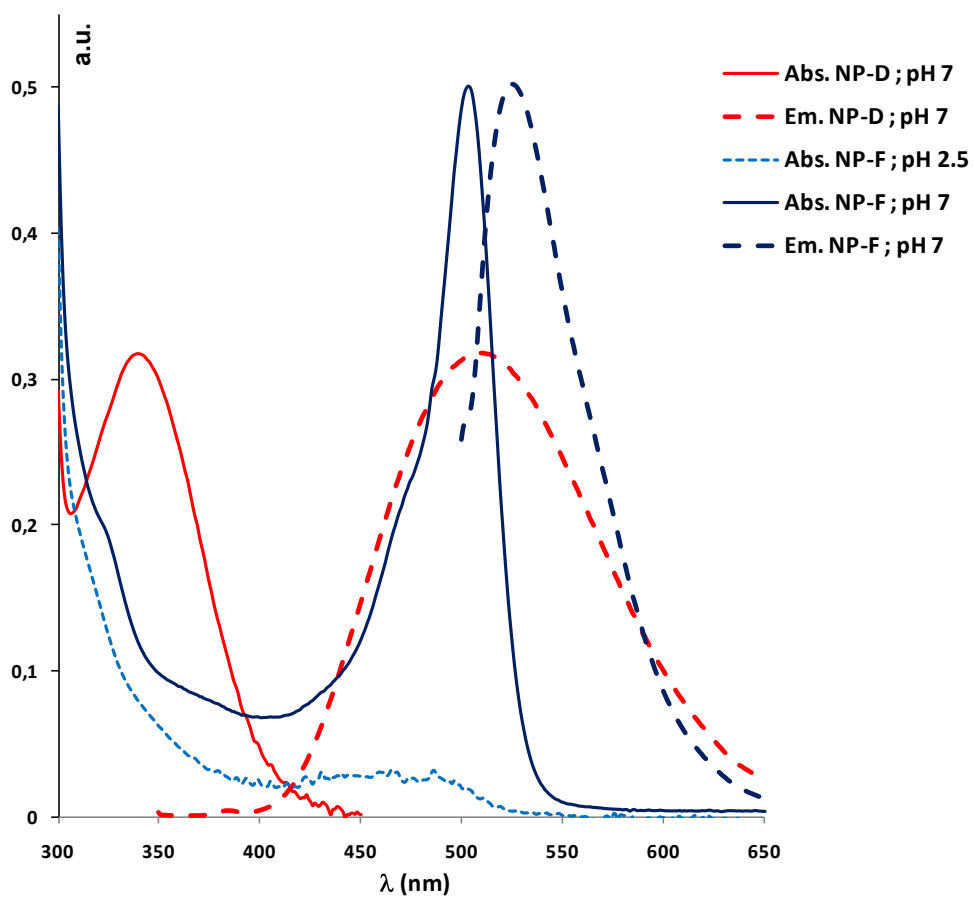
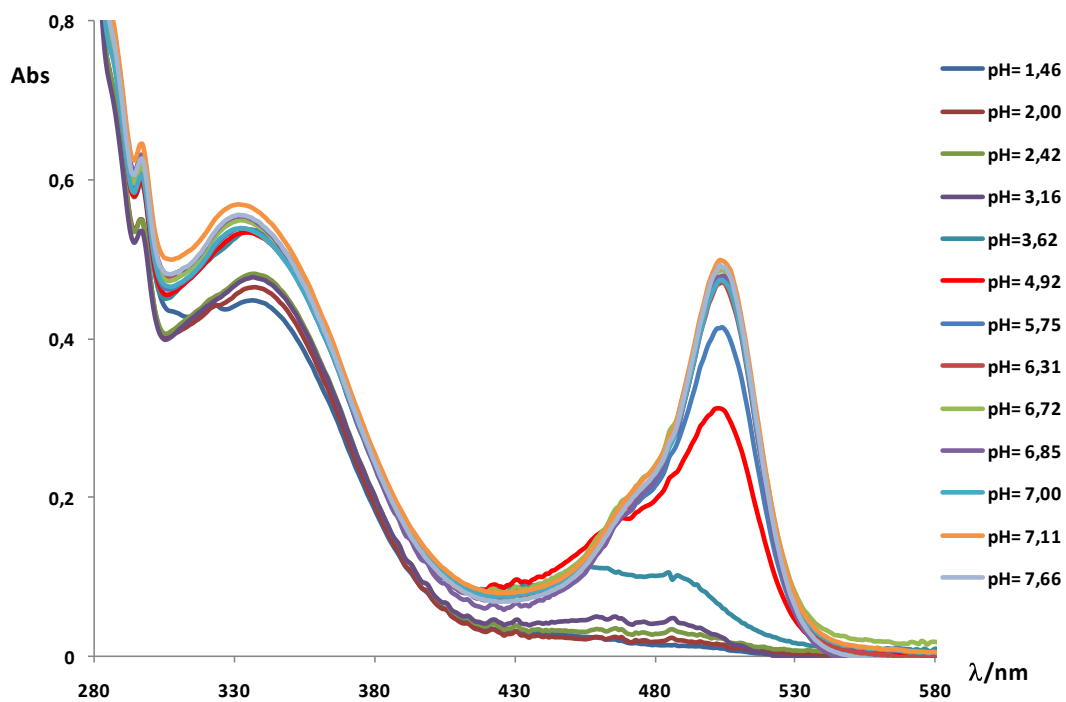
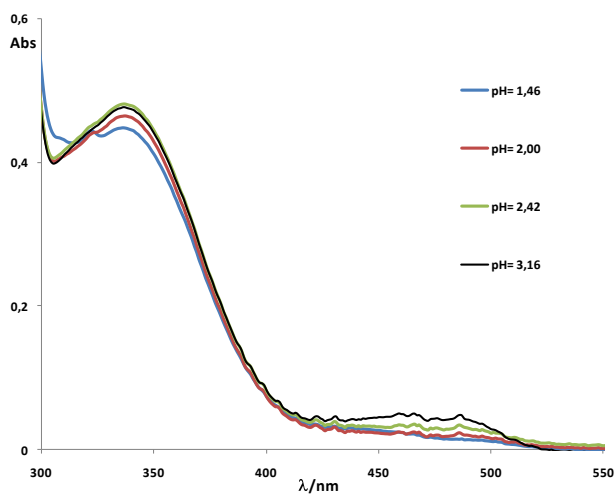


Figure S.7 : Absorption spectra of dual NPs NP-DF1 at different pH (suspension diluted 100 times in DTAB 0.5 wt%)

a) pH 1.5 to 7



b) pH 1.5 to 3.2



c) pH 3.6 to 7

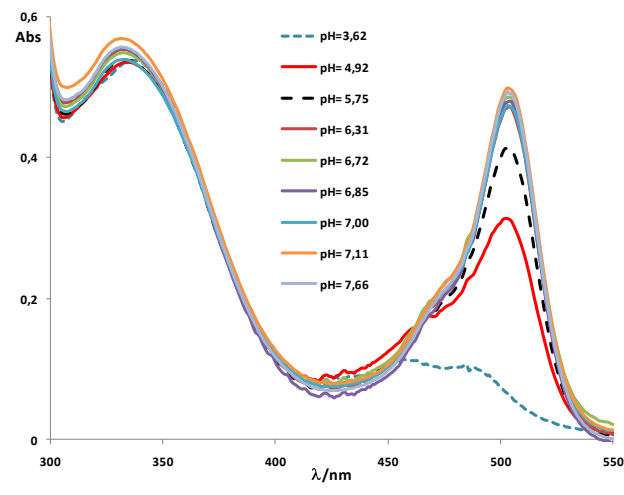
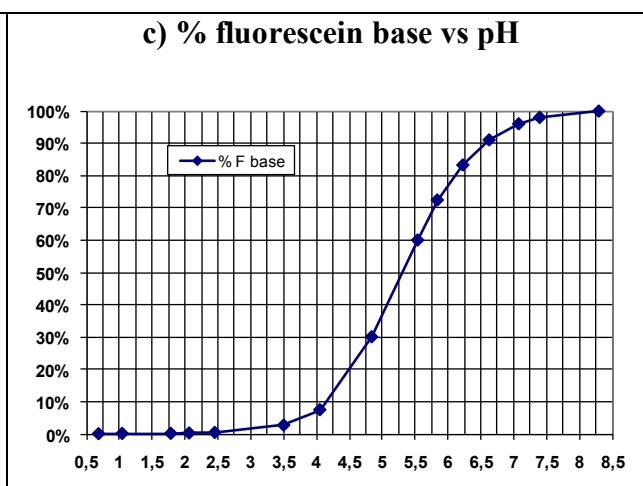
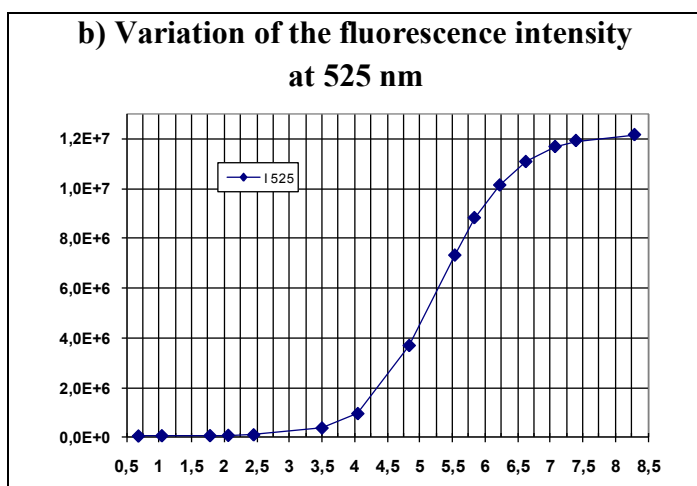
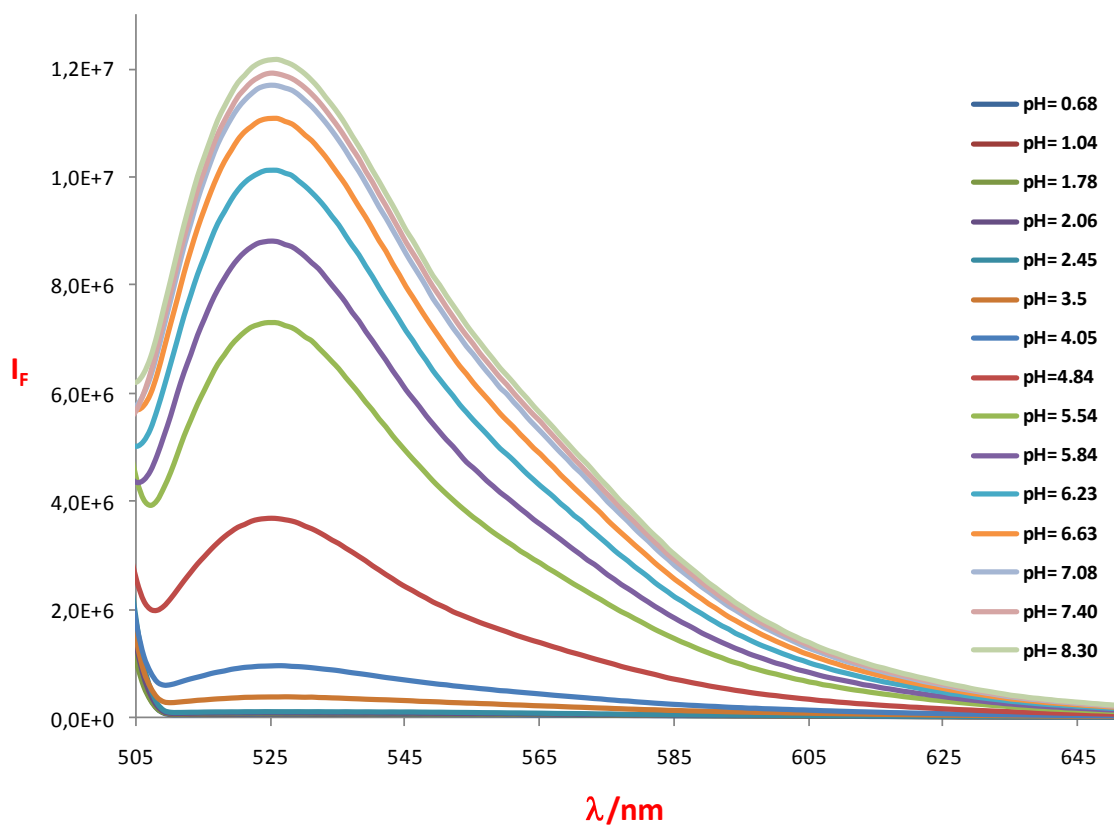


Figure S.8 : Fluorescence spectra of Dual NPs NP-DF1 at different pH values upon excitation of fluorescein at 500 nm (suspension diluted 1000 times in PBS 6 mM + DTAB 0.5 wt%)

a) Fluorescence spectra



Estimated pK value of fluorescein in NP-DF : 5.3

Figure S.9 : Fluorescence spectra of the aqueous suspension of Dual NP-DF1 upon excitation at 340 nm at different pH values (Dilution 1000 times in PBS 6mM + DTAB 0.5%wt)

a) pH 0.68 to 8.30

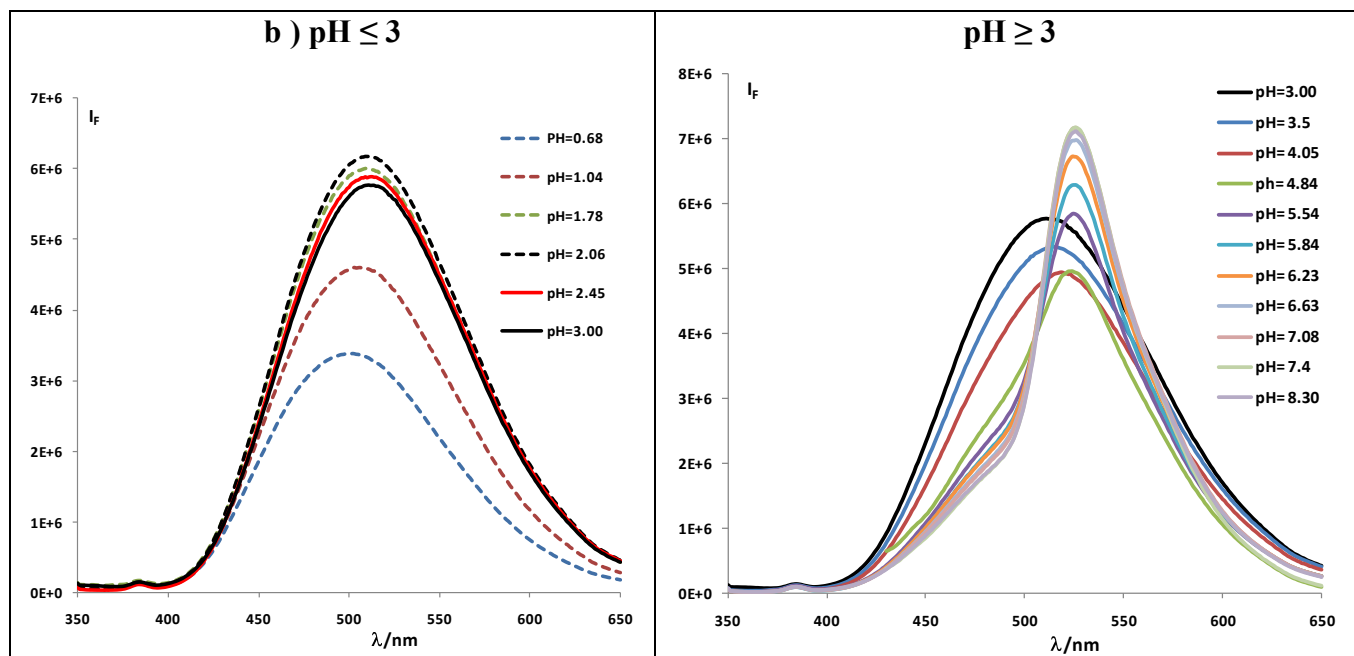
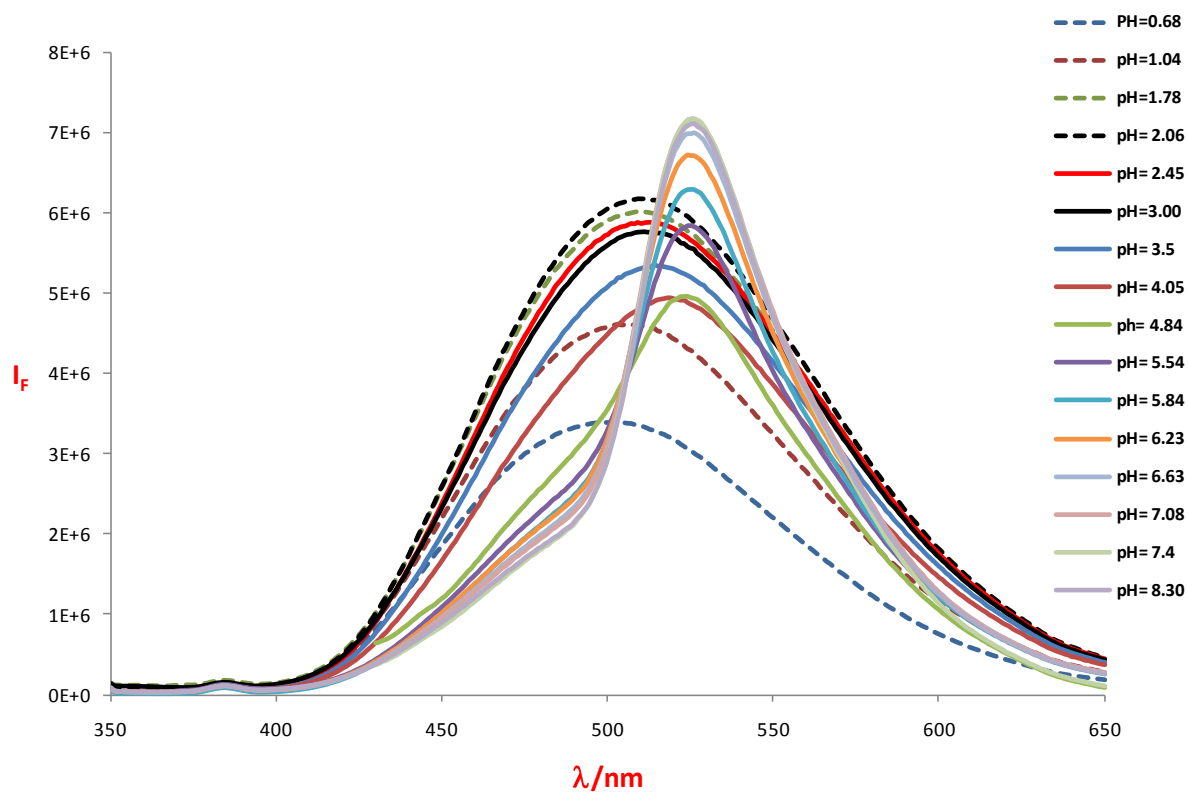
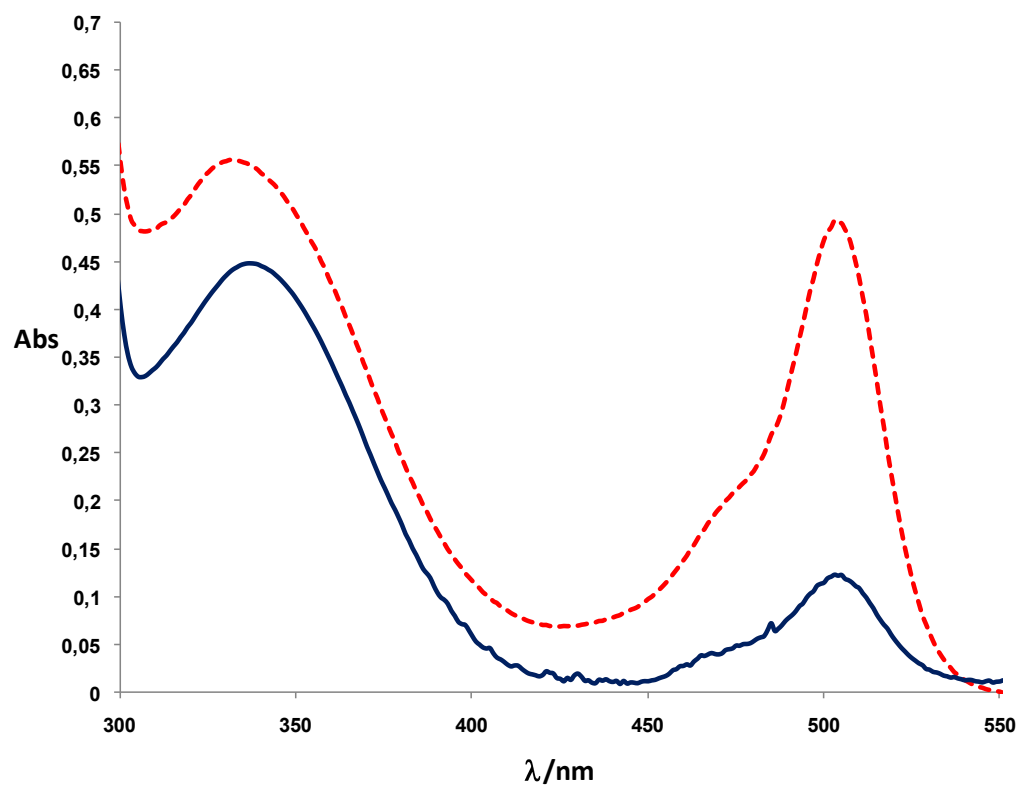


Figure S.10 : Absorption spectra of Dual NPs NP-DF1 and NP-DF2 at neutral pH (suspension diluted 100 times in DTAB 0.5 wt%)

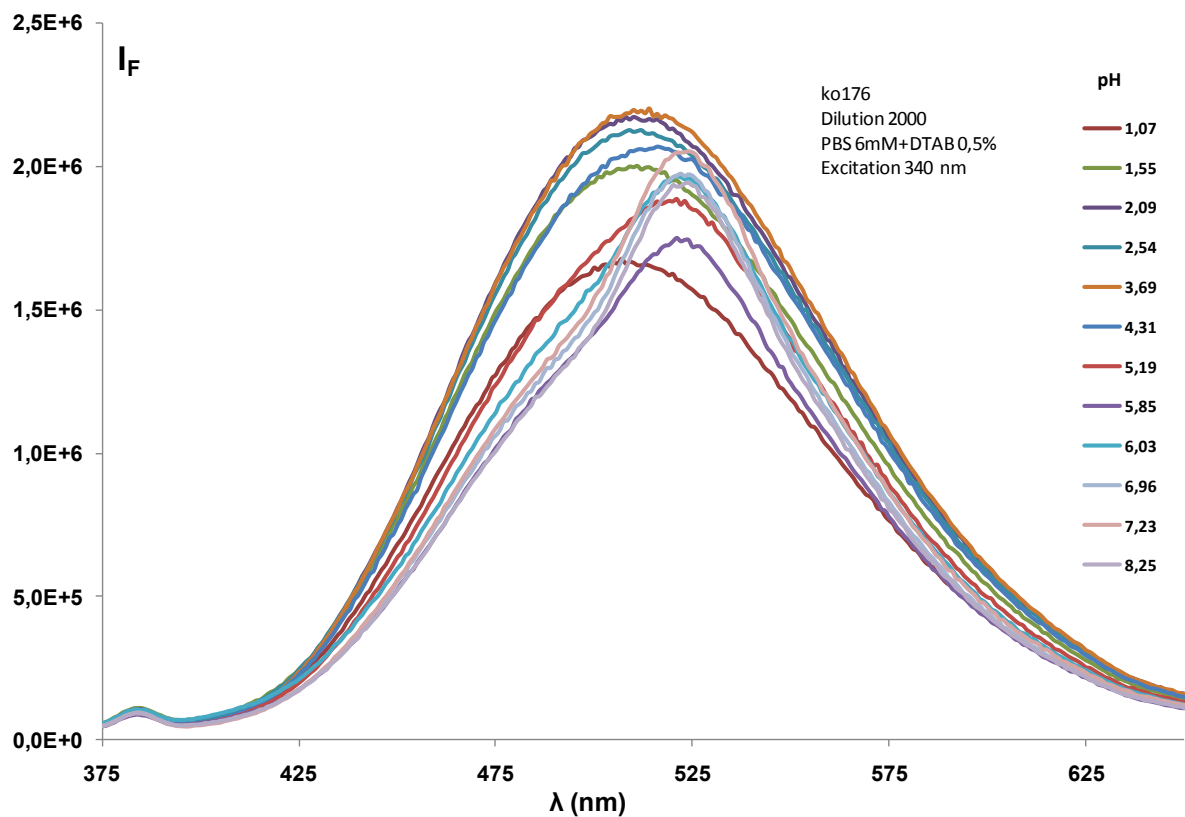


Dashed red line : NP-DF1 (pH 7.6)

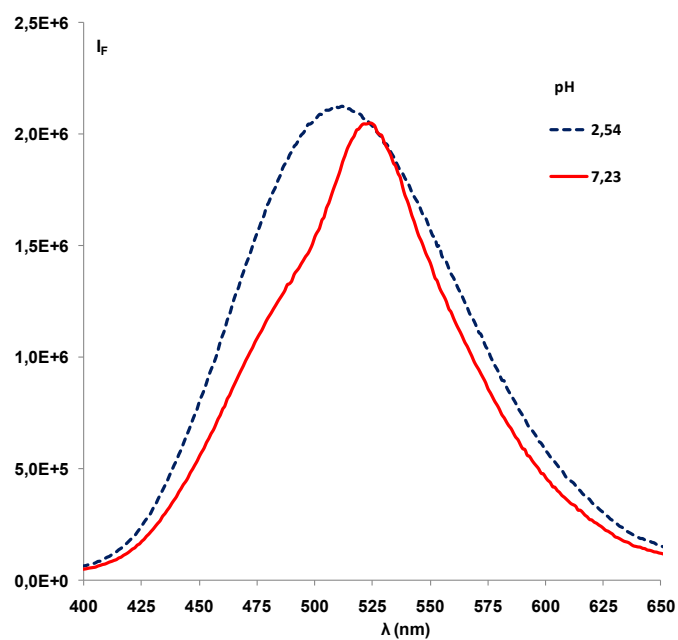
Blue solid line : NP-DF2 (pH 7.5)

Figure S.11 : Fluorescence spectra of the aqueous suspension of Dual NP-DF2 upon excitation at 340 nm at different pH values (Dilution 2000 times in PBS 6mM + DTAB 0.5%wt)

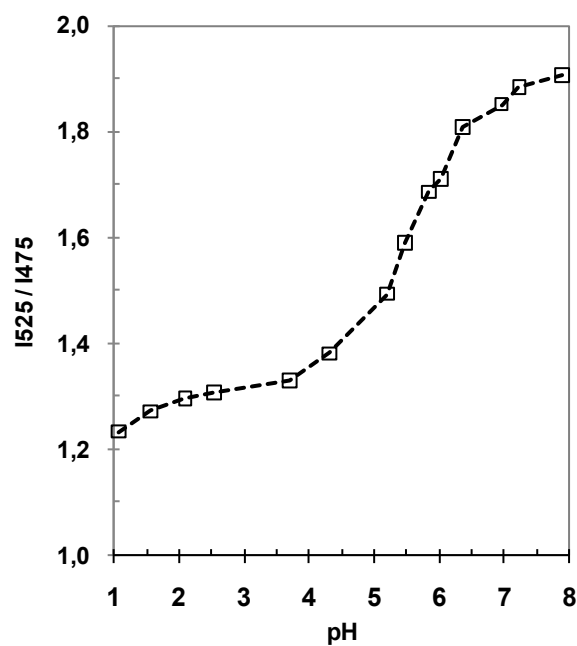
a) pH 1 to 8.2



b) Comparison of the fluorescence spectra at pH 2.5 and 7.2



c) I_{525}/I_{475} vs pH



Förster's distance R_0 and FRET efficiency

Förster's distance or critical distance R_0

The Förster's distance R_0 or critical distance is dependent on the spectral properties of the donor and acceptor molecules. R_0 is expressed as follows (eq. S.1):^{S4-S6}

$$R_0 = 0.2108 \times \kappa^2 \times n^{-4} \times \Phi_D \times \int_0^\infty J(\lambda) \epsilon_A(\lambda) d\lambda \quad \text{in Å} \quad (\text{eq. S.1})$$

κ^2 is the orientation factor for the emission and absorption dipoles and its value depends on their relative orientation, n is the refractive index of the medium and Φ_D is the quantum yield of the donor. $J(\lambda)$ is the overlap integral of the fluorescence emission spectrum of the donor and the absorption spectrum of the acceptor (eq. S.2).

$$J(\lambda) = \int_0^\infty I_D(\lambda) \times \epsilon_A(\lambda) \times \lambda^4 \times d\lambda \quad (\text{eq. S.2})$$

$I_D(\lambda)$ is the fluorescence intensity of the donor in the absence of acceptor, $\epsilon_A(\lambda)$ is molar extinction coefficient of the acceptor.

The approximate value of the Förster distance (R_0) has been calculated using photochemcad software from the emission and absorption spectra of **NP-D** and **NP-F** taking $\kappa^2 = 2/3$ (value for random orientation of the donor and acceptor molecules), $n = 1.57$, $\epsilon_A(\lambda) = 81100 \text{ L}\cdot\text{mol}^{-1}\cdot\text{cm}^{-1}$ (molar extinction coefficient of fluorescein base grafted on NPs in aqueous suspension)^{S7} and $\Phi_D = 0.03$ (reported value for N-propyldansylamide in water)^{S8} or $\Phi_D = 0.11$ (reported value for N-acetyldansylamide in acetonitrile/water 60/40).^{S9}

The calculated values are: $R_0 = 28 \text{ Å}$ for $\Phi_D = 0.03$ and $R_0 = 35 \text{ Å}$ for $\Phi_D = 0.11$.

FRET efficiency

Experimental energy transfer efficiencies E for different pH values were calculated from:

$$E = 1 - I_{475}/I_{\text{max},475} \quad (\text{eq. S.3})$$

where I_{475} is the emission intensity of Dansyl at a given pH and $I_{\text{max},475}$ is the maximum emission intensity of Dansyl (observed at pH = 2) at 475nm.

The variations of the dansyl emission intensity at 475 nm and of the experimental FRET efficiency as a function of pH for dual NPs, **NP-DF1** and **NP-DF2**, are presented in figure S.12.

According to the Förster non radiative energy transfer theory,^{S6b} the energy transfer efficiency E depends on the distance (d) between the donor (Dansyl) and the acceptor (Fluorescein base), on the critical energy transfer distance (R_0) and on the acceptor to donor ratio (m) expressed by the following relation (eq. S.4):

$$E = \frac{mR_0^6}{mR_0^6 + d^6} = \frac{m}{m + \left[\frac{d}{R_0}\right]^6} \quad (\text{eq. S.4})$$

m is the molar ratio of acceptor (fluorescein base : F base) to donor (unprotonated dansyl : Dns). The variation of m as a function of pH was determined from the concentrations of acceptor (F base) and donor (Dns) calculated using eq. S.5 and S.6, taking $F_{\text{tot}}/D_{\text{tot}}$ (overall fluorescein/Dansyl ratio on the NPs

surface) equal to 1/4 for **NP-DF1** and 1/13 for **NP-DF2** (as deduced from the absorption spectra and elemental analyses).

$$F_{\text{base}} = \frac{10^{-\text{pK}_F}}{10^{-\text{pK}_F} + 10^{-\text{pH}}} \times F_{\text{tot}} \quad (\text{eq. S.5}) \quad \quad \quad D_{\text{ns}} = \frac{10^{-\text{pK}_D}}{10^{-\text{pK}_D} + 10^{-\text{pH}}} \times D_{\text{tot}} \quad (\text{eq. S.6})$$

pK_F and pK_D are the pK_a values of fluorescein and dansyl, respectively. F_{tot} and D_{tot} are the overall concentrations of fluorescein and dansyl moieties grafted on the NPs surface.

The value of $\text{pK}_F = 5.3$ has been deduced from the variation of the emission spectra as a function of pH upon excitation at 500nm (figure S.8).

The value of pK_D has been estimated to be around 0.5 as deduced from the best fit of the variations of the relative dansyl emission at 475nm as a function of pH (*vide infra*, Figures S.14 and S.16).

The theoretical variations of the energy transfer efficiency as a function of pH have been calculated using equation S.4.

Theoretical variations of E as a function of pH for different values of d/R_0 are given in figure S.13a (**NP-DF1**) and figure S.15a (**NP-DF2**) and compared to the experimental variations of E for **NP-DF1** and **NP-DF2**.

The theoretical variations of the relative Dansyl emission intensity at 475 nm ($I_D/I_{D \text{ max}}$) as a function of pH have been deduced from the theoretical variations of E according to eq. S.3. The calculated variations for different values of pK_D and d/R_0 given in figures S.14a and S.16a show that the best fit with experimental data for **NP-DF1** and **NP-DF2** in the pH 0.5-3 range is obtained for an apparent pK_a value $\text{pK}_D=0.5$ of the dansyl units grafted on NPs.

To account for the experimental ET efficiencies lower than the calculated ones (63% compared to 94% for **NPDF1**; 34% compared to 52% for **NPDF2**), we calculated an effective ET efficiency $E_{\text{eff}} = 0.66 E$ as well as an effective $I_D/I_{D \text{ max}}$ deduced from E_{eff} .

Figures S.13b and S.15b show the calculated variations of E_{eff} vs pH for different values of d/R_0 compared to the observed variations in **NP-DF1** and **NP-DF2**. Figures S.14b and S.16b show the calculated variations of effective $I_D/I_{D \text{ max}}$ vs pH for different values of pK_D and d/R_0 compared to the observed variations in **NP-DF1** and **NP-DF2**.

For both NPs the best fits are obtained for $\text{pK}_D=0.5$.

For **NP-DF1** the best fits for E_{eff} and $I_D/I_{D \text{ max}}$ are obtained for $\text{pK}_D = 0.5$, $\text{pK}_F = 5.3$ and $d/R_0 = 0.5$ in good agreement with the estimated average dye-dye distance d in the order of 15 Å and the estimated value of R_0 in the order of 30 Å.

For **NP-DF2** the best fits for E_{eff} and $I_D/I_{D \text{ max}}$ are obtained for $\text{pK}_D = 0.5$, $\text{pK}_F = 5.3$ and $d/R_0 = 0.64$ in acceptable agreement with the estimated average dye-dye distance d in the order of 17 Å and the estimated value of R_0 in the order of 30 Å. This value of d/R_0 higher than the estimated one reflect the fact that at low acceptor to donor ratio the average distance between donor and acceptor residues is higher than the average overall distance between dyes residues grafted on the NP surface (*i.e.* the probability of one dansyl residue to have a neighbouring fluorescein residue is less than 1).

Förster's distance R_0 and efficiency for dansyl to dansyl FRET

The approximate value of the Förster distance ($R_{0\ Dns-Dns}$) for the dansyl/dansyl pair has been calculated as described above from the emission and absorption spectra of **NP-D** (fig. S. 6) taking $\varepsilon = 3960\ \text{L}\cdot\text{mol}^{-1}\cdot\text{cm}^{-1}$ and $\Phi_D = 0.11$ (reported values for N-acetyldansylamide in acetonitrile/water 60/40).^{S9}

The calculated value of $R_{0\ Dns-Dns} = 11\ \text{Å}$ indicates that energy transfer from a dansyl (donor) to another dansyl (acceptor) is effective for dansyl-dansyl distances up to $16.5\ \text{Å}$. Since the estimated average dye-dye distance on dual NPs is on the order of 15 and $17\ \text{Å}$, FRET from dansyl to dansyl can occur on the surface.

The FRET efficiency for a 1/1 dansyl pair at $d = 15\ \text{Å}$ is in the order of 15-20%. Actually on the NPs surface there is more than one neighbouring dansyl group. For instance in **NPDF1** (fluorescein/dansyl = 1/4), one dansyl unit is statistically surrounded by at least 3 other dansyl units (acceptor to donor ratio $m = 3$). The estimated FRET efficiency calculated using eq. S.4 is in the order 30%: it accounts quite well for the finding that 1 dansyl over 3 transfers to another dansyl rather than to fluorescein.

Figure S.12 : Variations of the emission intensity at 475 nm and FRET efficiency vs pH for dual NPs : NP-DF1 and NP-DF2

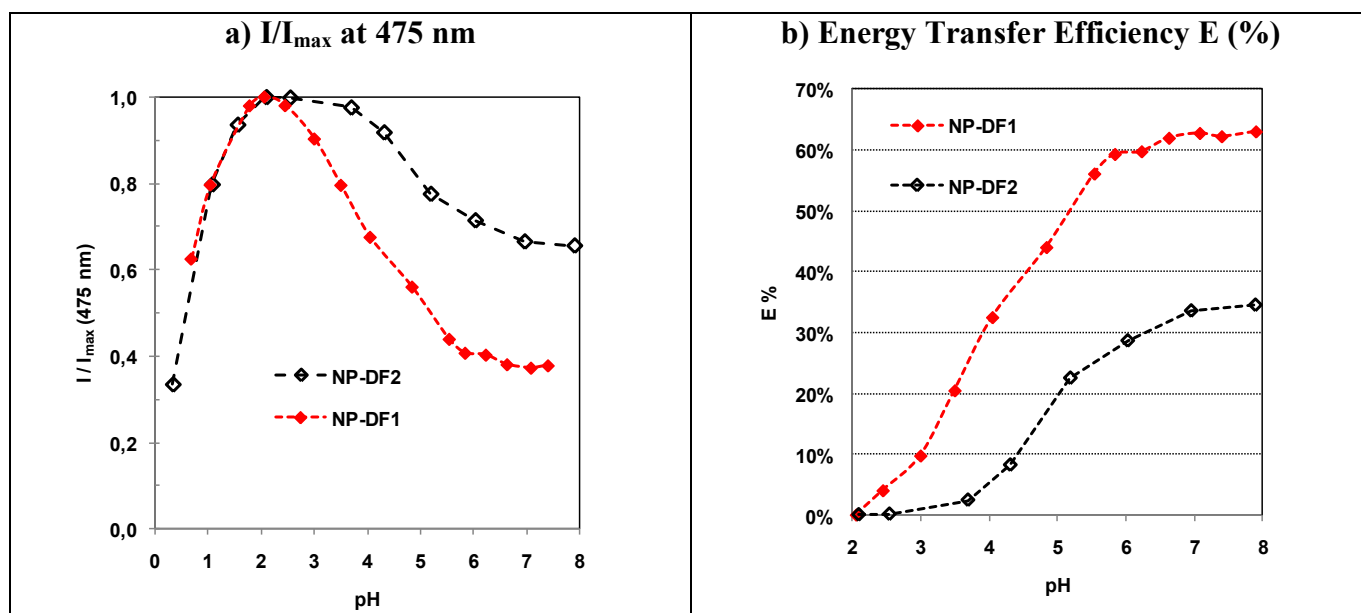
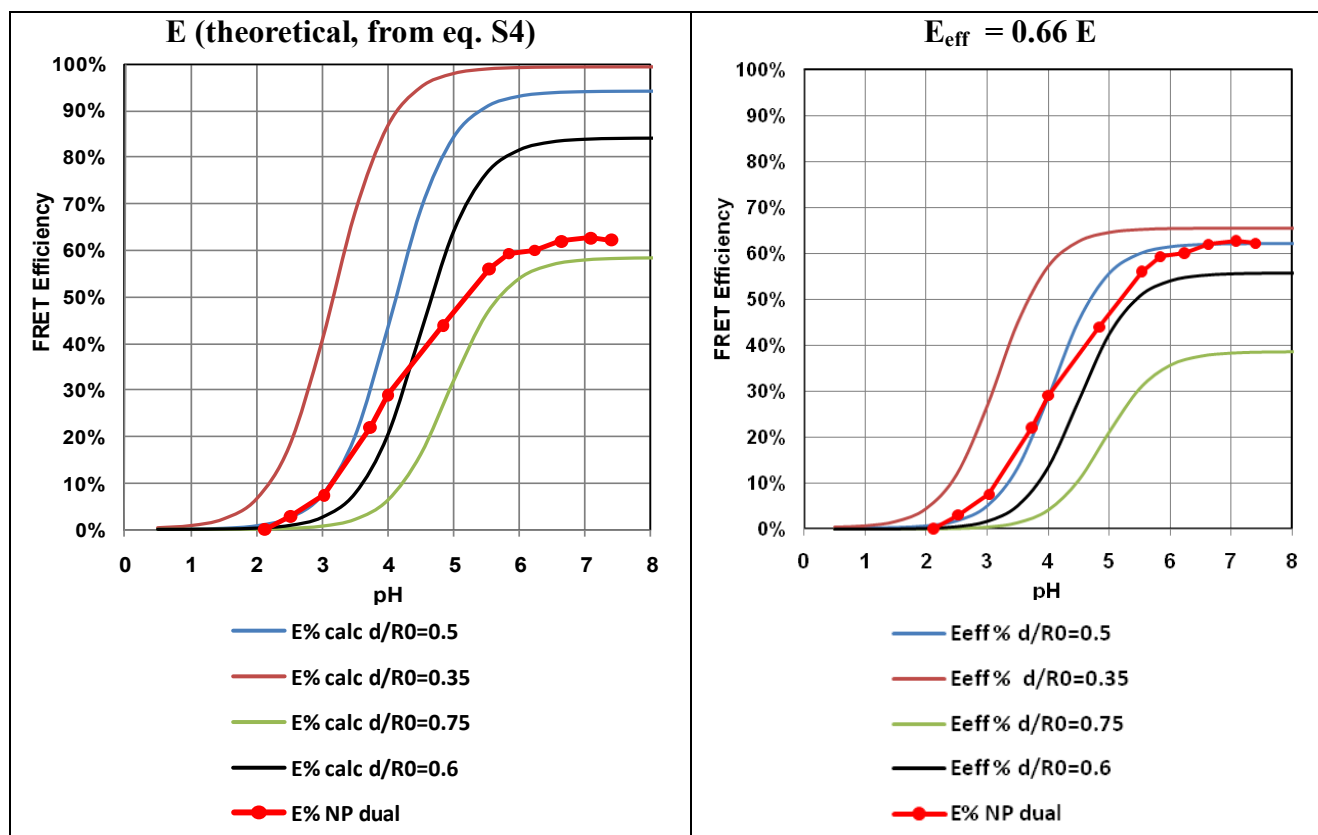


Figure S.13 : Calculated variations of E vs pH for different values of d/R_0 compared to the observed variations in NP-DF1.

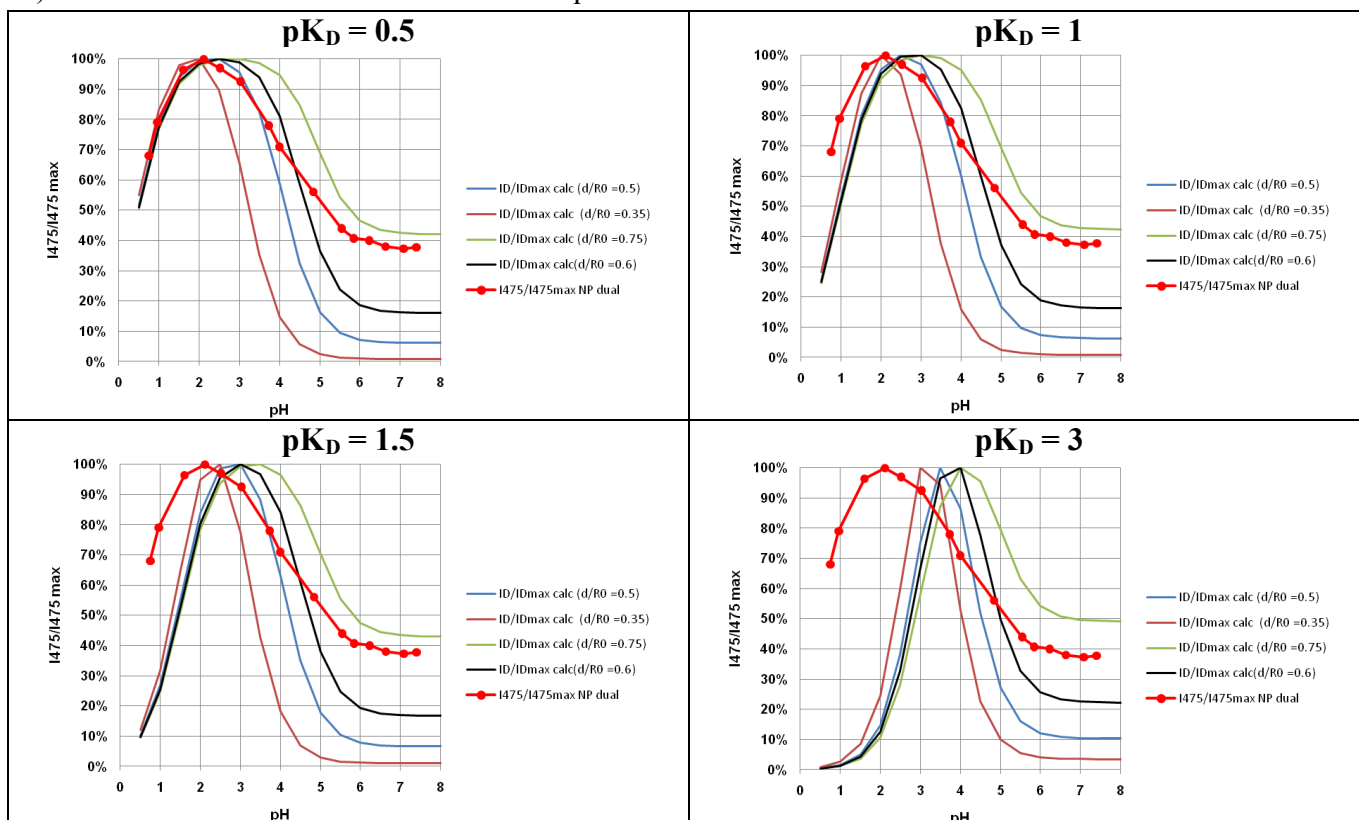


$$D/F = 4; pK_F = 5.3; pK_F = 0.5$$

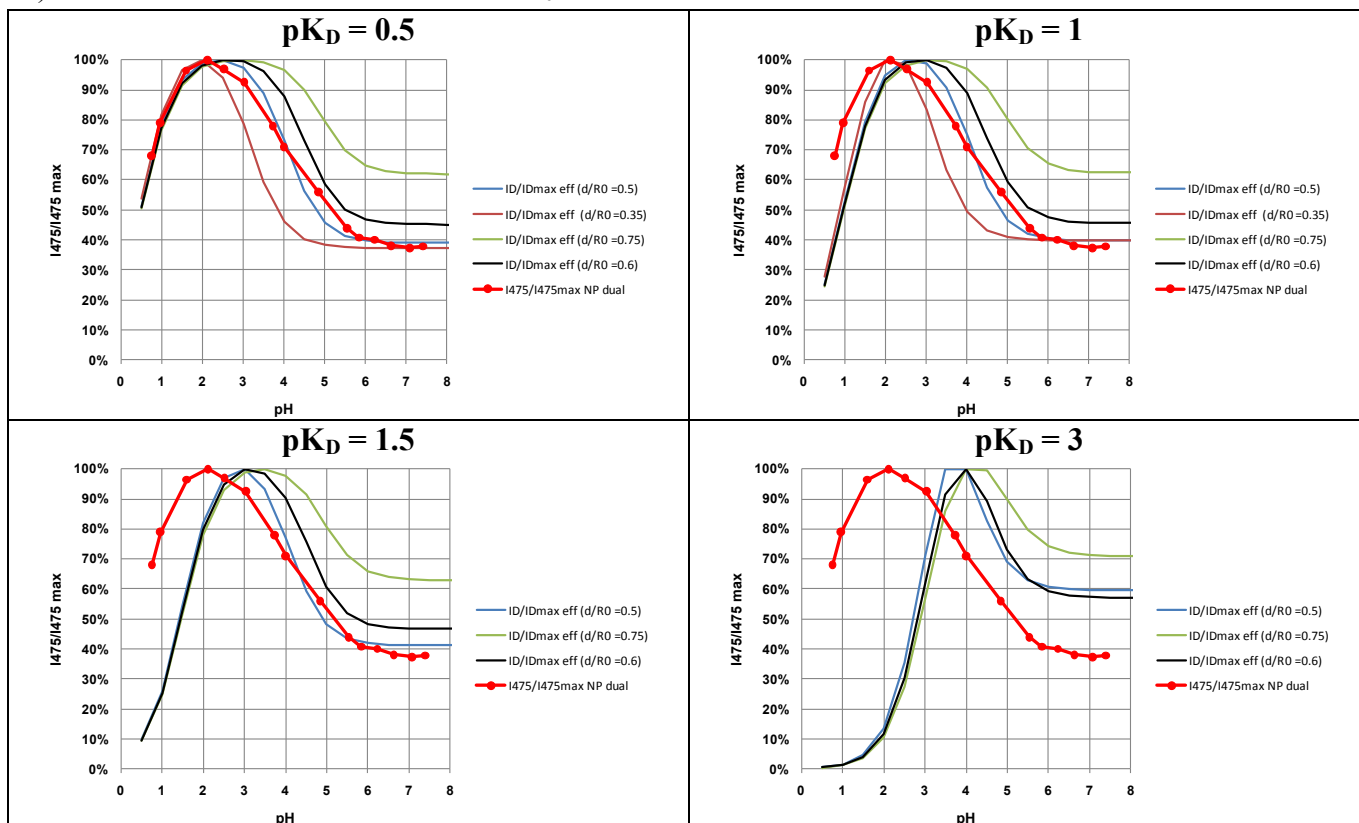
The best fit is obtained for $d/R_0 = 0.5$

Figure S.14 : Calculated variations of the relative emission of dansyl vs pH for different values of pK_D and d/R_0 compared to the observed variations in NP-DF1.

a) Theoretical variations calculated from eq. S4 and S3

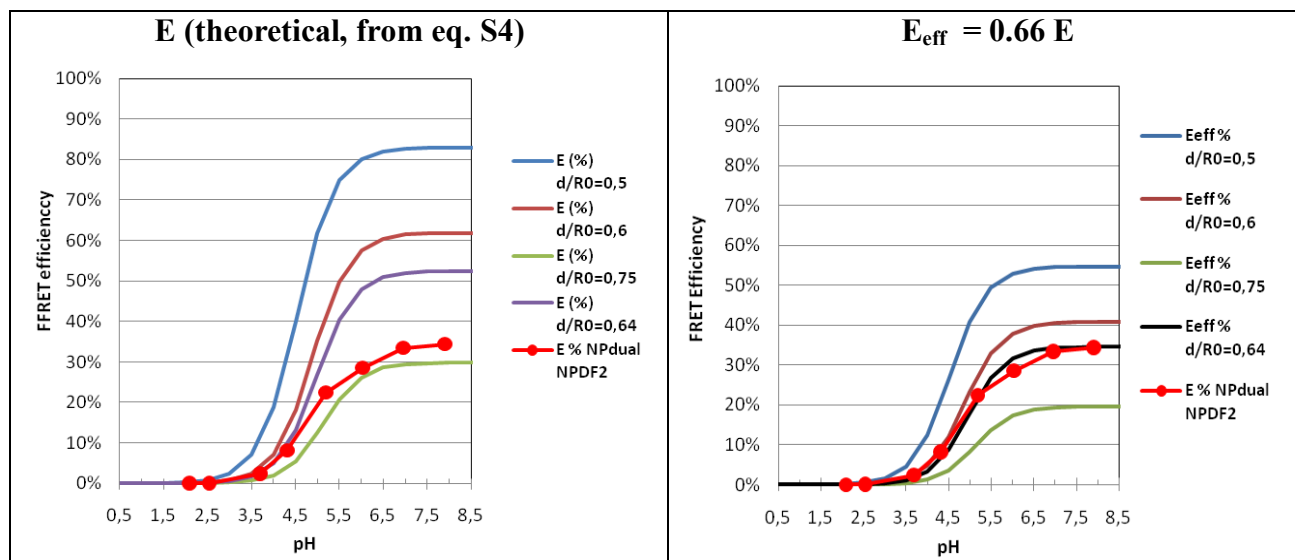


b) Effective variations calculated from E_{eff}



$D/F = 4$; $pK_F = 5.3$. The best fit is obtained for $d/R_0 = 0.5$ and $pK_D = 0.5$

Figure S.15 : Calculated variations of E vs pH for different values of d/R_0 compared to the observed variations in NP-DF2.

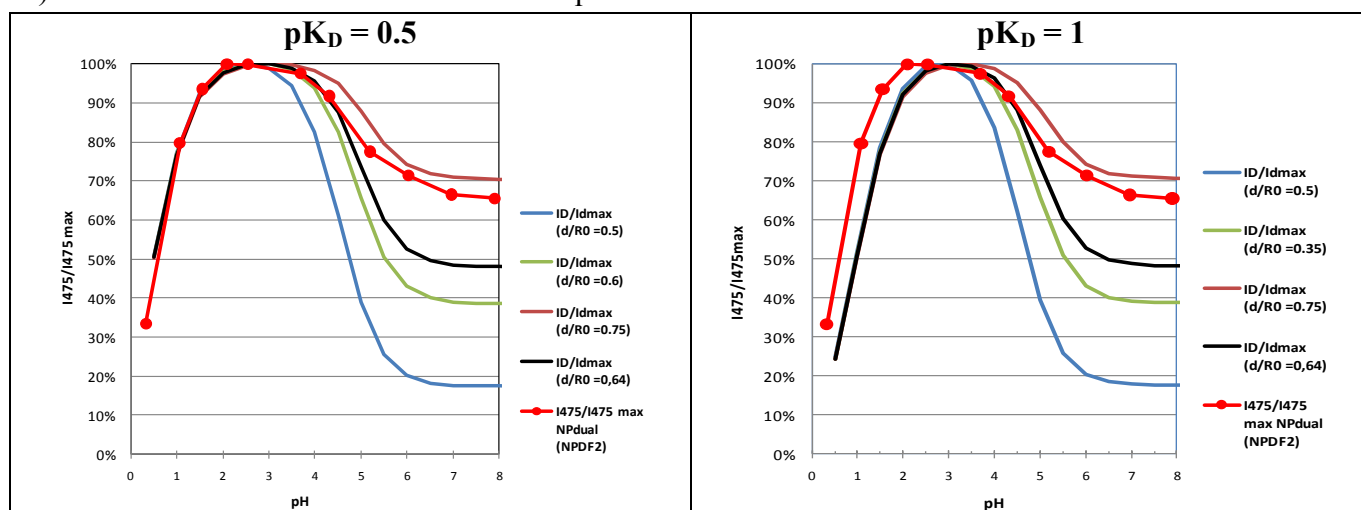


$$D/F = 13 ; pK_F = 5.3 ; pK_D = 0.5$$

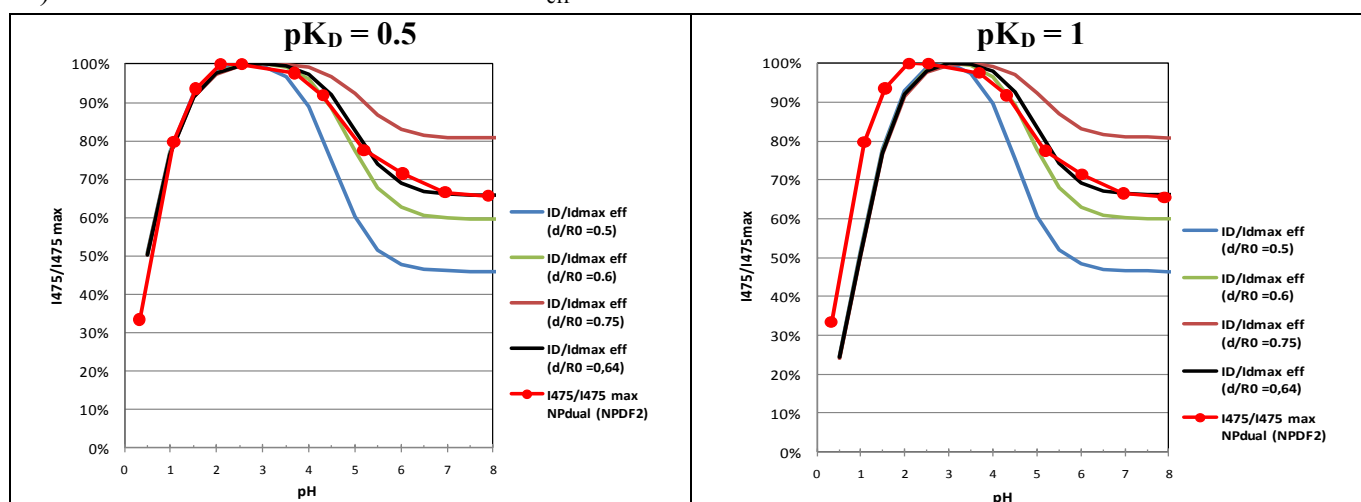
The best fit is obtained for $d/R_0 = 0.64$.

Figure S.16 : Calculated variations of the relative emission of dansyl vs pH for different values of pK_D and d/R_0 compared to the observed variations in NP-DF2.

a) Theoretical variations calculated from eq. S4 and S3



b) Effective variations calculated from E_{eff}



$D/F = 13$; $pK_F = 5.3$. The best fit is obtained for $d/R_0 = 0.64$ and $pK_D = 0.5$

References

- S1- F. Bolletta, D. Fabbri, M. Lombardo, L. Prodi, C. Trombini, N. Zaccheroni, *Organometallics* **1996**, *15*, 2415-2417.
 S2- B. P. Mason, S. M. Hira, G. F. Strouse, D. T. Mc Quade, *Org. Lett.* **2009**, *11*, 1479-1482.
 S3- a) C. Larpent, S. Amigoni-Gerbier, A. P. De Sousa Delgado, *C. R. Chim.* **2003**, *6*, 1275; b) F. Gouanvé, T. Schuster, E. Allard, R. Méallet-Renault, C. Larpent, *C. Adv. Funct. Mater.* **2007**, *17*, 2746.
 S4- J. R. Lakowicz, *Principles of Fluorescence Spectroscopy*; Plenum, New York, 1999.
 S5- B. Valeur in *Molecular Fluorescence: principles and applications*, Wiley-VCH, Weinheim, New York, **2002**.
 S6- a) K. E. Sapsford, L. Bert, I. L. Medintz, *Angew. Chem. Int. Ed.* **2006**, *45*, 4562-4588; b) A. R. Clapp, I. L. Medintz, H. Mattoussi, *ChemPhysChem* **2006**, *7*, 47-57.
 S7- E. Allard, C. Larpent, *J. Polym. Sci. Part A: Polym. Chem.* **2008**, *46*, 6206-6213.
 S8- M. Montalti, L. Prodi, N. Zaccheroni, G. Battistini, S. Marcuz, F. Mancin, E. Rampazzo, U. Tonellato, *Langmuir* **2006**, *22*, 5877-5881.
 S9- R. Métivier, I. Leray, B. Valeur, *Photochem. Photobiol. Sci.*, **2004**, *3*, 374-380.